Self-sensing paper-based actuators employing ferromagnetic nanoparticles and graphite

Hoang-Phuong Phan, Toan Dinh, Tuan-Khoa Nguyen, Ashkan Vatani, Abu Riduan Md Foisal (iD), Afzaal Qamar (iD), Atieh Ranjbar Kermany (iD), Dzung Viet Dao, and Nam-Trung Nguyen (iD)

View Online   Export Citation   CrossMark

ARTICLES YOU MAY BE INTERESTED IN

Tunable piezoresistive sensors based on pencil-on-paper
Applied Physics Letters 104, 073117 (2014); https://doi.org/10.1063/1.4866440

Ultra-high strain in epitaxial silicon carbide nanostructures utilizing residual stress amplification
Applied Physics Letters 110, 141906 (2017); https://doi.org/10.1063/1.4979834

A perspective on paper-based microfluidics: Current status and future trends
Biomicrofluidics 6, 011301 (2012); https://doi.org/10.1063/1.3687398

Self-sensing paper-based actuators employing ferromagnetic nanoparticles and graphite

Hoang-Phuong Phan,[a)] Toan Dinh, Tuan-Khoa Nguyen, Ashkan Vatani,
Abu Riduan Md Foisal, Afzaal Qamar, Atieh Ranjbar Kermany, Dzung Viet Dao,
and Nam-Trung Nguyen
Queensland Micro and Nanotechnology Centre, Griffith University, QLD 4111, Australia

Paper-based microfluidics and sensors have attracted great attention. Although a large number of paper-based devices have been developed, surprisingly there are only a few studies investigating paper actuators. To fulfill the requirements for the integration of both sensors and actuators into paper, this work presents an unprecedented platform which utilizes ferromagnetic particles for actuation and graphite for motion monitoring. The use of the integrated mechanical sensing element eliminates the reliance on image processing for motion detection and also allows real-time measurements of the dynamic response in paper-based actuators. The proposed platform can also be quickly fabricated using a simple process, indicating its potential for controllable paper-based lab on chip. *Published by AIP Publishing.* [http://dx.doi.org/10.1063/1.4979701]

Paper is a low cost and ubiquitous material that possesses various unique properties such as the ability to transport liquid, bio-compatibility, and biodegradability.[1,2] The lightness, flexibility, and specially worldwide availability also make paper a preferable choice for low-cost, portable, wearable, and printable electronics.[3–5] Utilizing these advantages, many paper-based applications have been developed including fuel cells, touching sensors, gas sensors, and microfluidics.[6–11] For instance, in the previous studies, we have demonstrated the use of porous paper as the substrate for wearable heaters as well as highly sensitive temperature sensors.[12–14] Paper has also been utilized as a low cost platform for the development of 3D scaffolds for cell growth and medical diagnostics devices.[15–19] Not only under research phase, numerous paper-based applications can be found in the market such as urine test strips and pregnancy test kits.[20,21]

In addition to paper-based sensors, it is desirable to have paper-based electrically controllable actuators as well because the prospect offers advantages such as the ability to manipulate the fluidic flow and to enable paper assembly. Whitesides group has recently pioneered in electro thermal paper actuators that can be controlled using thermal expansion of printed Poly(3,4-ethylenedioxythiophene) (PEDOT).[22] However, the high temperature of nearly $100\,^\circ$C required for the actuator could prevent it from niche applications that typically operate at room temperature. Additionally, to measure the motion of the actuator, a typical camera and image processing are required, which could make the system bulky and complex.[22,23] Consequently, a paper actuator with an integrated motion-sensing element is of interest to make it low-cost, compact, and electrically controllable.

This work presents the development of a self-sensing paper-based magnetic-actuator. The actuating component of the device was formed by employing nanoferromagnetic particles absorbed into porous paper. A graphite layer was used to create the mechanical sensing element for the paper-based

actuator. For the proof of concept, a cantilever-type device was fabricated using a clean-room free process, demonstrating the actuating and self-sensing functions integrated in a single paper-based device.

Figure 1 shows the concept of the proposed structure, which consists of (i) nanoferromagnetic particles for actuation and (ii) a graphite trace for deflection measurement. Ferro nanoparticles and a graphite trace are deposited on a typical printing paper through diffusion and mechanical friction, respectively. The actuator is driven by applying an external magnetic field generated from a permanent magnet or an electromagnet. Under the magnetic field, the ferro particles are attracted toward high magnetic potential, thus pulling the paper where these particles are embedded onto. In addition, the magnitude of actuation (e.g., elongation or deflection) can be controlled by changing the magnetic field. The motion detecting component is made of a graphite trace drawn on the paper. The deflection of the actuator results in a mechanical strain on the top surface of the paper, which changes the resistance of the graphite layer following its piezoresistive effect. Consequently, by measuring the resistance change of the graphite layer, the position as well as the speed of the actuator can be obtained. Therefore, the integration of the magnetically active ferro nanoparticles and strain-sensitive graphite allows the development of self-sensing paper-based actuators possible.

Figure 2 shows the fabrication process of the paper-based actuator. Starting from an A4 paper sheet ([TM]Staples) with a thickness of $110\,\mu$m, paper actuators are patterned into designed structures such as cantilevers, springs, and/or spirals using a laser cutter [TM]Speedy300 (step 1). The patterned paper is then dipped into a ferro fluid ([TM]EMG 707) for 30 s, allowing ferromagnetic nanoparticles to be deposited onto the porous networks of cellulose fibers (step 2). The volume concentration of ferromagnetic particles (C_{ff}) in EMG 707 was 2%, and the magnetic susceptibility of the fluid (X_{ff}) was 1.51. Subsequently, the dipped samples are dried out, using a hot plate at $60\,^\circ$C for 120 s, leaving the ferromagnetic particle on the paper (step 3). A graphite trace is

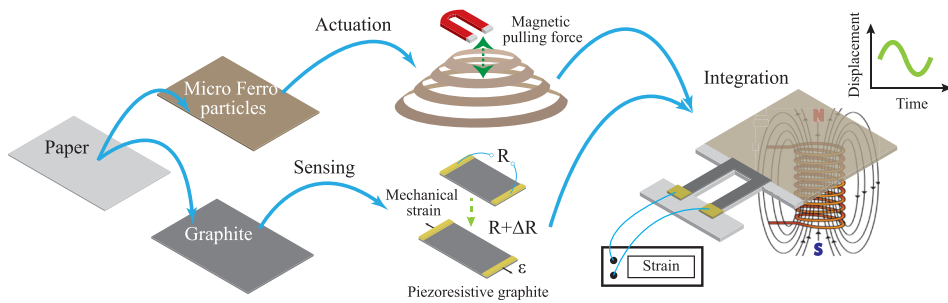[a)]Electronic mail: hoangphuong.phan@gri_thuni.edu.au

FIG. 1. Concept of the sensing integrated paper-based actuator. The device is actuated by the magnetic pulling force, while its displacement is obtained based on the piezoresistance of a graphite layer deposited on the surface of paper.

then hand-drawn on the paper, forming the strain sensing element for the actuator (step 4). We chose a 5B grade pencil ([TM]Faber-Castell) to create the graphite trace as it offers a high content of graphite of approximately 82 wt. %, thus providing a relatively large electrical conductivity. Electrical contact and wiring were then created using highly conductive silver epoxy ([TM]RS Components 1863616).

We initially characterized the piezoresistive effect of graphite trace for the subsequent motion sensing. The properties of graphite trace were investigated using the Raman scattering measurements ([TM]Renishaw inVia Raman microscope 514 nm), Fig. 3(a). Evidently, three prominent peaks at 1350, 1580, and 2725 cm^{-1} were observed, which correspond to the D, G, and 2D bands, respectively. Furthermore, the average grain size (L) of the graphite material can be estimated from the integrated intensities of the D and G bands reported by Cancado *et al.*:[24] $L = 2.4 \times 10^{-10} \times A^4 \times (I_D/IG)^{-1}$, where λ is the wavelength of the laser source in the Raman measurement and I_D/I_G is the ratio between the intensities of the D and G bands. Accordingly, the crystalline grain-size of the graphite trace was approximately 45 nm.

The mechanical properties of the paper were characterized using the bending beam method.[25] For the sake of simplicity, a rectangular-shaped paper cantilever with dimensions of 40 mm × 15 mm × 0.11 mm was utilized in this experiment. The cantilever was fixed at one end using an acrylic clamp, while the other end was deflected. The deflection of the cantilever was measured using a 3-dimensional micro-manipulator ([TM]Cascade Microtech PH110). The applied force was measured using a precise electronic scale ([TM]AND FX300i) (detailed in the supplementary material). The

relationship between the Young's modulus (E) and the deflection (d) of a paper cantilever is

$$E = \frac{4Fl^3}{wh^3d},\tag{1}$$

where l, w, and h are the length, width, and thickness of the paper cantilever, respectively. Figure 3(b) shows the relationship between the applied force and the deflection of the paper cantilever. Accordingly, the Young's modulus of the paper was found to be 3.2 GPa, which is in agreement with other results.[26,27]

Next, the magnitude of the piezoresistive effect in the as-fabricated graphite trace was investigated by monitoring its resistance change under mechanical impacts. A schematic sketch of the self-sensing cantilever used in this experiment is shown in Fig. 3(c), where the graphite trace was formed at the supporting hinges. The deflection at the free end of the cantilever was applied and measured using the aforementioned micro-manipulator. The resistance change of the graphite trace was converted into an output voltage using a Wheatstone bridge and a voltage amplifier ([TM]AD623),[28] Fig. 3(c). Figure 3(d) presents the output of the graphite resistor under a mechanical load at the free end of the cantilever. Accordingly, when the cantilever is deflected 2 mm downward, a relatively large voltage of 2.5 V was observed. The output voltage then returned to almost 0 when the applied force was completely removed. The relative resistance
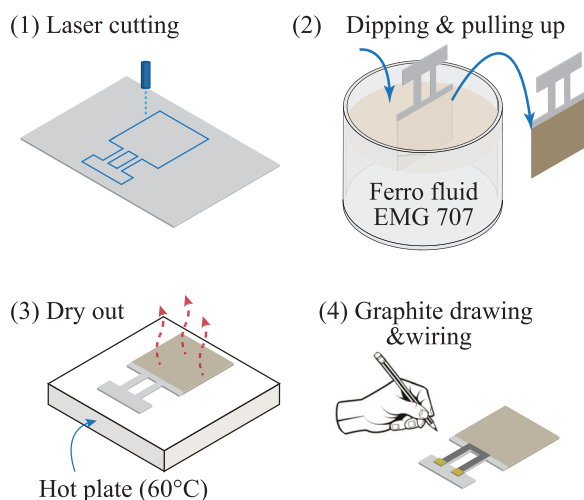

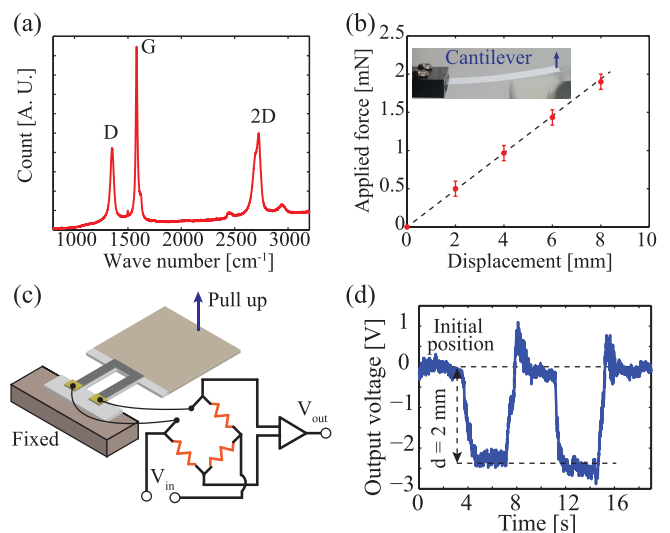FIG. 2. Fabrication process of a self-sensing paper-based actuator.

FIG. 3. Characterization of the piezoresistive effect in graphite on paper. (a) The Raman spectroscopy of 5B graphite; (b) Young's modulus measurement of paper; (c) The resistance-to-voltage converting circuit; and (d) The output voltage of graphite piezoresistor under applied forces.

change ($\Delta R/R$) of graphite was derived from the output voltage:[29] $\Delta R/R = (4\Delta V/V_{in})/G$, where $V_{in} = 5$ V was the input voltage and $G = 400$ was the amplified gain. The gauge factor of the piezoresistance in graphite is quantified as: $GF = (\Delta R/R)/\varepsilon$, where ε was the applied strain, which was estimated using the Finite element analysis (FEA) simulation. It should also be pointed out that the Young's modulus of the paper with the graphite trace drawn on its surface was found to be almost the same as that of the initial material (i.e., $E = 3.2$ GPa). This result is reasonable since the graphite trace was only deposited on the top surface of paper. Therefore, from Fig. 3, the gauge factor of 5B graphite was found to be approximately 10. The long term stability of the graphite sensors was characterized by applying the bending test for 1000 cycles, indicating an excellent stability with a small deviation of below 2% (detailed in the supplementary material).

The piezoresistive effect in the graphite trace is considered to be caused by the change in grain distance under mechanical strain. The relationship between the resistance of graphite and tunneling distance (t) is $R(t) \propto e^{\beta t}$, where β is a

function of the potential height and t is the distance between graphite grains.[30,31] The tunneling distance between graphite grains is changed to ($t + \delta t$) under applying strain, resulting in a change in the tunneling resistance: $R(t + \Delta t) \propto e^{\beta(t + \delta t)}$. Using this numerical analysis, the gauge factor of 5B graphite was estimated to be within 10–15, which was in solid agreement with our experimental data.[30] Based on the piezoresistive effect of the graphite trace, it is possible to obtain the position of the paper actuator by monitoring the response of the graphite resistor under actuation.

Figure 4 presents the demonstration of magnetic paper actuators with the integrated strain sensing element. The cellulose network of a typical A4 paper was clearly observed using scanning electron microscopy (SEM). In addition, it is also evident from the SEM images that magnetic nanoparticles are placed in the porous areas between the cellulose fibers, as shown in Fig. 4(a). Furthermore, since paper is a flexible material that can be easily deflected and folded, it is possible to fabricate magnetic paper actuators with a high degree of freedom. A demonstration of magnetic paper
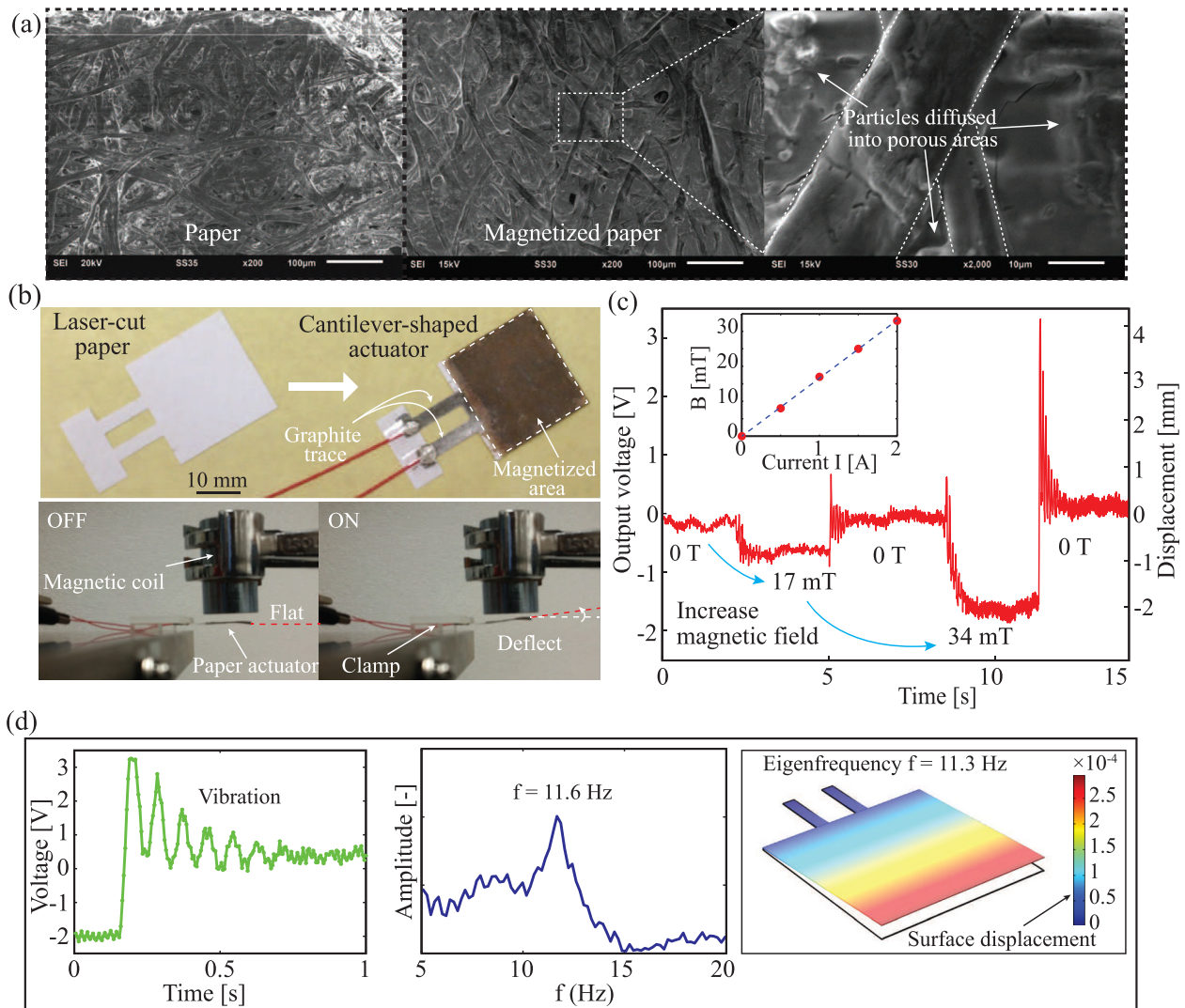

FIG. 4. Demonstration of the paper-based actuator driven by magnetic force and sensed by the piezoresistive effect. (a) SEM images of an A4 paper (left) and magnetized paper (middle and right); (b) Photograph of the as-fabricated paper actuator and its deflection under external magnetic field. (c) Displacement measurement of the self-sensing paper actuator utilizing the piezoresistive effect in the graphite layer drawn on the hinges (Inset: The relationship between the applied current and the magnetic field density B); and (d) Measurement of the resonant frequency of the cantilever actuator using the piezoresistance of graphite (left: output voltage plotted in time-domain; middle: Fourier transform; and right: FEA simulation).

actuators with different types of motions is presented in the supplementary material.

Figure 4(b) presents the photographs of a cantilever-shaped self-sensing actuator with strain sensing element integrated into its hinge parts. The deflection of the cantilever-shaped actuator under applied magnetic field can also be clearly observed. Figure 4(c) shows the performance of the cantilever-shaped actuator. To actuate this cantilever-shaped paper actuator, a magnetic field generated from a home-built electromagnetic coil was employed. The magnitude of the magnetic field could be controlled by modifying the current applied to the coil, thus changing the pulling-force exerting on the ferromagnetic particles, Fig. 4(d) Inset. Employing the piezoresistance of graphite from the previous experiment, the deflection of a cantilever actuator is plotted in Fig. 4(d). Accordingly, increasing the external magnetic strength results in a larger displacement of the paper actuator. The actuator also returned to its initial position when the external magnetic field is switched off. Since both actuating and position-sensing mechanisms are based on electrically driven-systems, no optical measurement setup is required, making our proposed structure suitable for fully electrically controllable paper-based devices. The relationship between applied magnetic field and the displacement of the actuator also allows a quantitative estimation of the density of the ferromagnetic particles absorbed into paper. The magnetic susceptibility of a nanoferro particle (χ_p) can be assumed as:[32] $\chi_p = \chi_{ff}/C_{ff} = 1.51/2\% = 75$. The magnetic force exerted on each nanomagnetic particle is[33]

$$F_p = \mu_0 V_p (M_p \cdot \nabla H_a), \qquad (2)$$

where $\mu_0 = 4\pi \times 10^{-7}$ H/m is the magnetic constant, $V_p = (4/3)\pi r^3$ is the volume of a particle with a radius of $r = 5$ nm, $M_p = \chi_p H_a/(1 + \chi_p/3)$ is the magnetization of a particle, and H_a is the applied magnetic field strength. Consequently, the driving magnetic force (F) of the cantilever actuator is (supplementary material)

$$F = N_p V F_p, \qquad (3)$$

where N_p is the density of the magnetic particles and $V = W \times H \times L$ is the volume of paper that absorbs the nanomagnetic particles (W, H, and L are the width, thickness, and length of the square area of the fabricated magnetic actuator, respectively). Consequently, from Fig. 4 and Eqs. (2) and (3), the magnetic particle concentration was found to be $N_p = 2.65 \times 10^{17}$ cm^{-3}. This density of nanoparticles is considerably high owing to the nature of porous paper which allows the particles to diffuse deeply into the paper.

Furthermore, the use of electrical measurement (i.e., the piezoresistive effect in graphite) also allows real time monitoring of the dynamic motion of the paper-based actuator, without the need for a complicated optical system and post-image processing. Figure 4(d) shows a damped vibration of the magnetic paper actuator. An impulse magnetic field was applied, causing the cantilever to deflect. Once the magnetic field is switched off, the cantilever actuator keeps vibrating due to the energy stored in the spring. From the response of the graphite trace, the resonance frequency of the cantilever

was obtained using the Fourier transform. Accordingly, the resonant frequency of the cantilever was found to be 11.6 Hz. This result was consistent with the FEA frequency estimation shown in Fig. 4(d), in which the Young's modulus of magnetized paper was set at 3.4 GPa, the Poisson's ratio of the paper was 0.2, and the mass densities of the initial paper and magnetized paper were 800 kg/m^3, and 850 kg/m^3, respectively.[34] This capability of measuring dynamic response can be utilized to develop a wide range of paper-based mechanical sensors including mass detections and flow sensors.

In conclusion, we developed cost-effective paper actuators where ferromagnetic nanoparticles and graphite trace can be easily trapped on papers using extremely simple techniques such as dipping and drawing. The actuating force can be controlled by modifying the applied magnetic field, while the deflection of the actuator can be measured using the piezoresistance of graphite, demonstrating the electrically controllable capability in the fabricated paper-based actuator. The proposed platform shows its potential for fully integrated paper-based microfluidics and soft robotics.

See supplementary material for the experimental setup for Young's modulus measurement of paper in Fig. 3, the experimental data of long term stability test of graphite piezoresistors, the demonstration with magnetic actuators with different shapes, and the derivation of Eq. (3).

[1]K. Yamada, T. G. Henares, K. Suzuki, and D. Citterio, Angew. Chem. **54**, 5294 (2015).

[2]X. Li, D. R. Ballerini, and W. Shen, Biomicrofluidics **6**, 011301 (2012).

[3]S. K. Mahadeva, K. Walus, and B. Stoeber, Appl. Mater. Interfaces **7**, 8345–8362 (2015).

[4]A. W. Martinez, S. T. Phillips, G. M. Whitesides, and E. Carrilho, Anal. Chem. **82**, 3–10 (2010).

[5]L. Nyholm, G. Nystrom, A. Mihranyan, and M. Stromme, Adv. Mater. **23**, 3751–3769 (2011).

[6]P.-K. Yang, Z.-H. Lin, K. C. Pradel, L. Lin, X. Li, X. Wen, Jr.-H. He, and Z. L. Wang, ACS Nano **9**, 901 (2015).

[7]F. Guder, A. Ainla, J. Redston, B. Mosadegh, A. Glavan, T. J. Martin, and G. M. Whitesides, Angew. Chem. **128**, 5821 (2016).

[8]S. Chen, Q. Wan, and A. K. Badu-Tawiah, J. Am. Chem. Soc. **138**(20), 6356 (2016).

[9]X. Liao, Q. Liao, X. Yan, Q. Liang, H. Si, M. Li, H. Wu, S. Cao, and Y. Zhang, Adv. Funct. Mater. **25**, 2395–2401 (2015).

[10]C.-W. Lin, Z. Zhao, J. Kim, and J. Huang, "Pencil drawn strain gauges and chemiresistors on paper," Sci. Rep. **4**, 3812 (2014).

[11]Y. Wang, H. Guo, J.-J. Chen, E. Sowade, Y. Wang, K. Liang, K. Marcus, R. R. Baumann, and Z.-S. Feng, ACS Appl. Mater. Interfaces **8**, 26112–26118 (2016).

[12]T. Dinh, H.-P. Phan, D. V. Dao, P. Woodfield, A. Qamar, and N.-T. Nguyen, J. Mater. Chem. C **3**, 8776–8779 (2015).

[13]T. Dinh, H.-P. Phan, A. Qamar, N.-T. Nguyen, and D. V. Dao, RSC Adv. **6**, 77267–77274 (2016).

[14]T. Dinh, H.-P. Phan, T.-K. Nguyen, A. Qamar, A. R. M. Foisal, T. N. Viet, C. D. Tran, Y. Zhu, N.-T. Nguyen, and D. V. Dao, J. Mater. Chem. C **4**, 10061–10068 (2016).

[15]J. T. Connelly, J. P. Rolland, and G. M. Whitesides, Anal. Chem. **87**, 7595 (2015).

[16]A. Nemiroski, D. C. Christodouleas, J. W. Hennek, A. A. Kumar, E. J. Maxwell, M. T. Fernandez-Abedul, and G. M. Whitesides, Proc. Natl. Acad. Sci. U. S. A. **111**, 11984 (2014).

[17]B. Mosadegh, M. R. Lockett, K. Thu, K. A. Simon, K. Gilbert, S. Hillier, D. Newsome, H. Li, A. B. Hall, D. M. Boucher, B. K. Eustace, and G. M. Whitesides, Biomaterials **52**, 262 (2015).

[18]S. Burnham, J. Hu, H. Anany, L. Brovko, F. Deiss, R. Derda, and M. W. Griffiths, Anal. Bioanal. Chem. **406**, 5685 (2014).

[19]A. K. Yetisen, M. S. Akram, and C. R. Lowe, Lab Chip **13**, 2210–2251 (2013).

[20]J. Hu, S. Wang, L. Wang, F. Li, B. Pingguan-Murphy, T. J. Lu, and F. Xu, Biosens. Bioelectron. **54**, 585–597 (2014).

[21]P. Von Lode, Clin. Biochem. **38**, 591–606 (2005).

[22]M. M. Hamedi, V. E. Campbell, P. Rothemund, F. Guder, D. C. Christodouleas, J.-F. Bloch, and G. M. Whitesides, Adv. Funct. Mater. **26**, 2446–2453 (2016).

[23]M. Amjadi and M. Sitti, ACS Nano **10**, 10202–10210 (2016).

[24]L. G. Cancado, K. Takai, T. Enoki, M. Endo, Y. A. Kim, H. Mizusaki, and M. A. Pimenta, Appl. Phys. Lett. **88**, 163106 (2006).

[25]H.-P. Phan, T. Kozeki, T. Dinh, T. Fujii, A. Qamar, Y. Zhu, T. Namazu, N.-T. Nguyen, and D. V. Dao, RSC Adv. **5**, 82121–82126 (2015).

[26]X. Liu, M. Mwangi, X. Li, M. O'Briena, and G. M. Whitesides, Lab Chip **11**, 2189 (2011).

[27]M. Khoury, G. E. Tourtollet, and A. Schroder, Ultrasonics **37**(2), 133–139 (1999).

[28]H.-P. Phan, T. Dinh, T. Kozeki, T. K. Nguyen, A. Qamar, T. Namazu, N.-T. Nguyen, and D. V. Dao, IEEE Electron Device Lett. **37**, 1029–1032 (2016).

[29]D. V. Dao, H.-P. Phan, A. Qamar, and T. Dinh, RSC Adv. **6**, 21302–21307 (2016).

[30]T.-K. Kang, Appl. Phys. Lett. **104**, 073117 (2014).

[31]S. Kanaparthi and S. Badhulika, Nanotechnology **27**, 095206 (2016).

[32]Z. M. Wang, R. G. Wu, Z. P. Wang, and R. V. Ramanujan, Sci. Rep. **6**, 26945 (2016).

[33]E. P. Furlani, J. Appl. Phys. **99**, 024912 (2006).

[34]K. Schulgasser, Fibre Sci. Technol. **15**, 257–270 (1981).